



# Four-Component Synthesis of 2-Amino-3-Cyanopyridine Derivatives Catalyzed by Cu@imineZCMNPs as a Novel, Efficient and Simple Nanocatalyst Under Solvent-Free Conditions

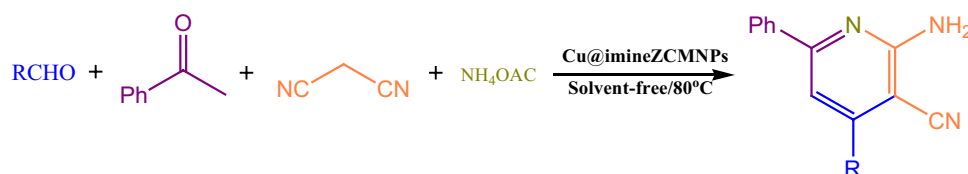
Asieh Yahyazadeh<sup>1</sup> · Esmayeel Abbaspour-Gilandeh<sup>1</sup> · Mehraneh Aghaei-Hashjin<sup>2</sup>

Received: 8 November 2017 / Accepted: 28 January 2018  
© Springer Science+Business Media, LLC, part of Springer Nature 2018

## Abstract

An efficient and convenient method was investigated for synthesis of 2-amino-3-cyanopyridine derivatives via a one-pot four-component reaction of various types of aldehydes, acetophenone, malononitrile, and ammonium acetate in the presence of 10 mg Cu@imineZCMNPs catalyst. The favorable products were achieved with high quantitative yields and easy isolation of products in short reaction times under solvent-free conditions. The prepared catalytic system was characterized by Fourier transform infrared spectroscopy, energy dispersive X-ray, thermogravimetric analysis, X-ray diffraction, transmission electron microscopy, scanning electron microscopy and vibrating sample magnetometer. Due to the magnetic nature of the catalyst, it can be easily recovered by an external magnetic field and comfortable reused.

## Graphical Abstract



**Keywords** Heterogeneous catalyst · 2-Amino-3-cyanopyridine · Solvent-free conditions · Reusable catalyst · Multicomponent reaction · Vibrating sample magnetometer

## 1 Introduction

The use of nanocatalysts in various organic reactions is an interesting procedure to achieve green catalysis, which is suitable for the environment and is of high interest in various processes of chemical transformations which happened by catalysis in heterogeneous conditions. During recent years, the preparation of catalysts based on magnetic nanoparticles, because of reasons such as the avoidance of tedious

separation methods through distillation or extraction, has attracted high consideration in the synthetic chemistry, pharmaceutical industry and technology fields and only negligible changes in their selectivity and activity supplied the possibility of their reuse [1–6].

The molecules containing pyridine moiety such as 2-amino-3-cyanopyridines has a wide pharmaceutical and biological activities, such as IKK- $\beta$ -inhibitors, A<sub>2A</sub> adenosine receptor antagonists, antimicrobial, antiviral, antibacterial, antitumor, antifungal, antihypertensive, as well as anti-inflammatory properties [7–14]. Numerous protocols have been reported for the production of 2-amino-3-cyanopyridines that some of these procedures need long reaction times, toxic solvent, high temperature, microwave or ultrasound irradiation and multiple steps [15–19]. Hence, it

✉ Asieh Yahyazadeh  
yahyazadeh@guilan.ac.ir

<sup>1</sup> Chemistry Department, University of Guilan,  
Rasht 41335-1914, Iran

<sup>2</sup> Young Researchers and Elites Club, Ardabil Branch, Islamic  
Azad University, Ardabil, Iran

**Scheme 1** Cu@imineZCMNPs catalyzed synthesis of 2-amino-3-cyanopyridines

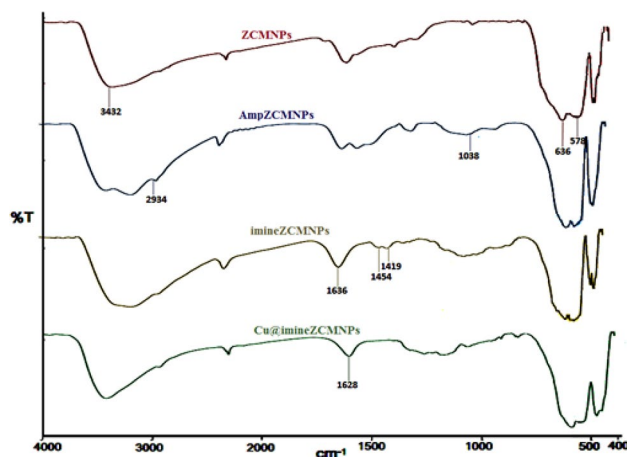
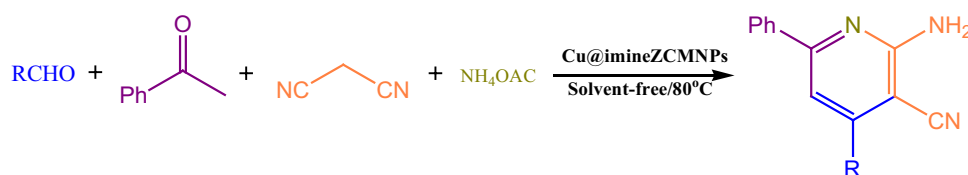


**Fig. 1** FTIR spectra of ZCMNPs, AmpZCMNPs, imineZCMNPs and Cu@imineZCMNPs

is essential to expand an improved path for the synthesis of 2-amino-3-cyanopyridines under mild reaction conditions.

In continuation of our efforts to the synthesis of new catalysts for organic transformations [20–24], we decided to investigate the synthesis of 2-amino-3-cyanopyridine derivatives with various substituents from the reaction of aldehyde, acetophenone, malononitrile and ammonium acetate under solvent-free conditions using Cu@imineZCMNPs as a novel, eco-friendly, reusable and promising nanocatalyst (Scheme 1).

## 2 Results and Discussion

The infrared spectra of the ZCMNPs, AmpZCMNPs, imineZCMNPs and Cu@imineZCMNPs samples in the region of 400–4000  $\text{cm}^{-1}$  are exhibited in Fig. 1. In the spectrum of the ZCMNPs, the observed peak at 578  $\text{cm}^{-1}$  correspond to the Fe-O stretching frequency and a strong broadband at 3435  $\text{cm}^{-1}$  is related to the OH groups attached to the iron. Appearance absorption band at 636  $\text{cm}^{-1}$  in the spectra is attributed to Zr-O groups, indicating magnetite nanoparticles functionalization has been done successfully. In the spectrum of pure AmpZCMNPs, the observed peak at 1038  $\text{cm}^{-1}$  is related to the stretching vibration of the Si-O groups while the peaks appearing in the 2934  $\text{cm}^{-1}$  region can be attributed to the aliphatic C-H stretching vibration mode. The 1419 and 1454  $\text{cm}^{-1}$  bands in the imineZCMNPs

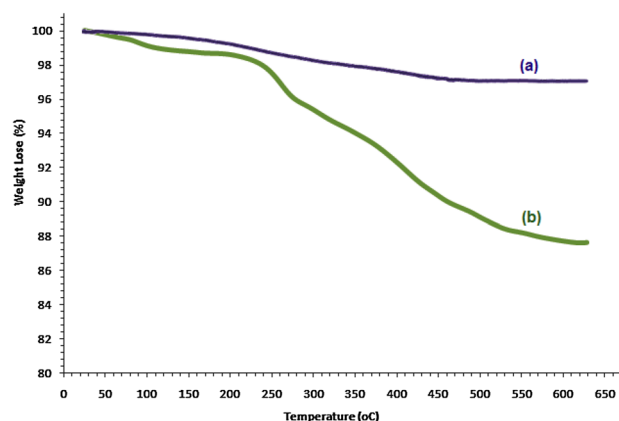


**Fig. 2** TGA curves of **a** MNPs and **b** Cu@imineZCMNPs

have been collectively assigned to the stretching vibration of the C=C bond. Also, the presence of stretching vibrations band in 1636  $\text{cm}^{-1}$  is attributed to the imine C=N group. It should be noted that the C=N signal of the Cu@imineZCMNPs is shifted to a lower wavenumber than the C=N stretching frequency of imineZCMNPs (1628  $\text{cm}^{-1}$  rather than 1636  $\text{cm}^{-1}$ ). It is indicating that C=N bond is coordinated to Cu metal through the lone pair of nitrogen.

Thermogravimetric analysis (TGA) of MNPs and Cu@imineZCMNPs was proved the presence of organic compounds on the surface of magnetite nanoparticles (Fig. 2). The TGA curve of MNPs demonstrates a weight loss of approximately 5% up to a temperature of 430  $^{\circ}\text{C}$ , which is concerned with the loss of the adsorbed water as well as dehydration of the surface OH groups (Fig. 2a). TGA of Cu@imineZCMNPs illustrates two considerable weight loss steps due to the decomposition of the organic part of aminopropyl and salicylaldehyde (Fig. 2b).

The XRD patterns of MNPs, imineZCMNPs and Cu@imineZCMNPs represents diffraction peaks corresponding to the cubic spinel phase of magnetic iron oxide nanoparticles (JCPDS card No. 79-0417) and no peak dedicated to Cu species appeared in the patterns of Cu@imineZCMNPs compared those of imineZCMNPs, probably due to the tiny size of Cu species (Fig. 3). This clearly illustrates that the cubic spinel phase of imineZCMNPs remained intact upon metal incorporation.

The surface morphology, size distribution and particle shape of the Cu@imineZCMNPs were examined by scanning electron microscopy (SEM) as shown in Fig. 4a. The

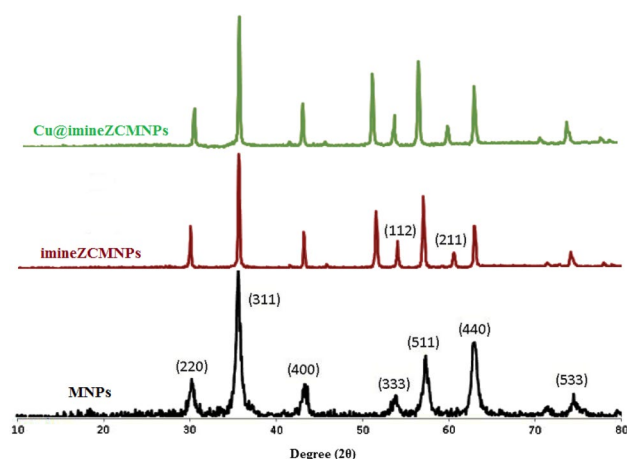


**Fig. 3** XRD patterns of MNPs, imineZCMNPs and Cu@imineZCMNPs

SEM image of the Cu@imineZCMNPs clearly indicates variations in the surface of these nanoparticles. The SEM image shows that these nanoparticles are of nearly spherical morphology with mean diameter of about 48 nm. In the case of recycled Cu@imineZCMNPs after the fifth cycle of the reaction, the SEM image shown negligible change in the size (56 nm) or morphology of the catalyst nanoparticles (Fig. 4b).

The TEM images of Cu@imineZCMNPs determined that it appears to have an almost spherical shape with a narrow size distribution (the average particle size is 30 nm, Fig. 5), thereby retaining a nanocrystalline appearance. Therefore, the great active sites of this nanocatalyst may allow for high activity in organic transformations, even with a low catalyst loading.

Energy dispersive X-ray (EDX) mapping was performed to verify the composition of the Cu@imineZCMNPs nanocatalyst (Fig. 6). The EDX analysis illustrated the existence of copper, iron, carbon, zirconium and silicon in the structure of Cu@imineZCMNPs catalyst that approved catalyst preparation successfully. Also, the content of Cu in Cu@imineZCMNPs was determined by Inductively coupled

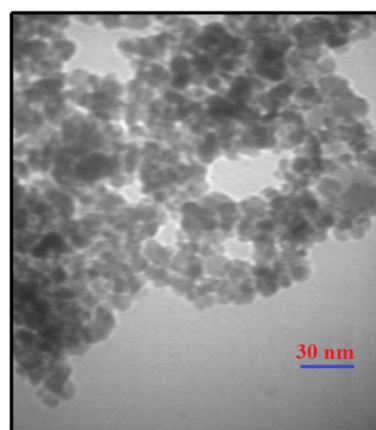


**Fig. 5** TEM images of Cu@imineZCMNPs

plasma atomic emission spectrometry (5.2% of Cu anchored on catalyst).

The magnetic feature of the catalyst, which accounts for its easy recovery, was surveyed with a vibrating sample magnetometer (VSM) at room temperature. Figure 7 shows the magnetization diagram for the bare MNPs and Cu@imineZCMNPs with the field sweeping from  $-8500$  to  $+8500$  Oersted. The saturation magnetization value of Cu@imineZCMNPs nanoparticles emerged to be 39.86 emu/g, which are much lower than the bare MNPs (61.22 emu/g) [25].

### 3 Screening of Reaction Conditions

In order to screen the reaction conditions for the synthesis of 2-amino-4,6-diphenyl-nicotinonitrile (1a), a systematic study considering different variables affecting the reaction yield was investigated in a condensation reaction of benzaldehyde (1 mmol), acetophenone (1 mmol), malononitrile (1 mmol), and ammonium acetate (1.5 mmol) as a model reaction under solvent-free conditions. The results are listed in Table 1. The initial optimization experiments revealed that the desired product 1a was formed after 1 h in only 18%

**Fig. 4** SEM images of Cu@imineZCMNPs (a) and recycled Cu@imineZCMNPs (b)

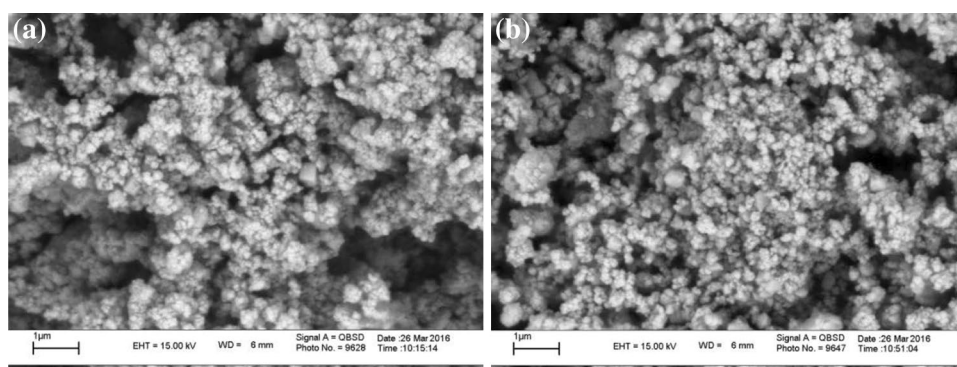


**Fig. 6** EDX spectrum of prepared Cu@imineZCMNPs nanocatalyst

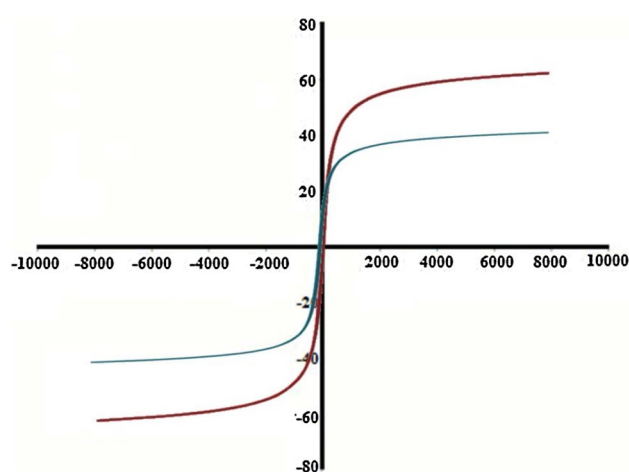
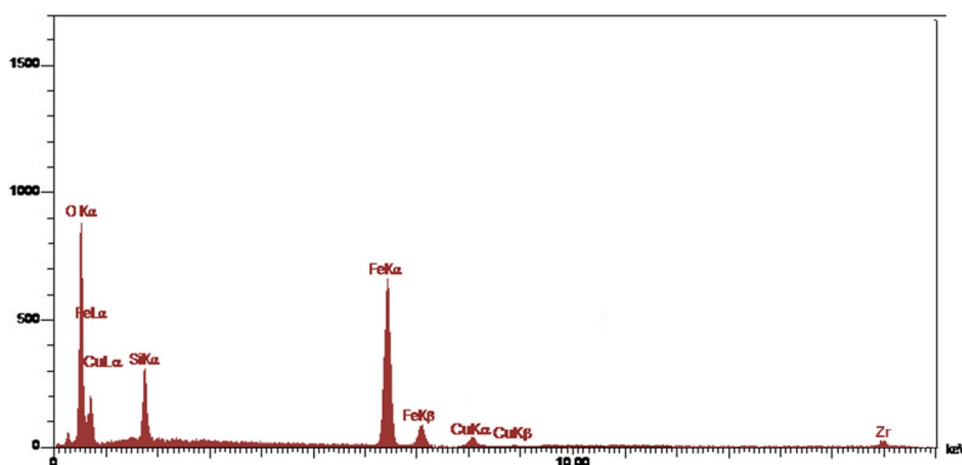


**Fig. 7** VSM magnetization curves of the bare MNPs and Cu@imineZCMNPs

yield (entry 1). Moderate yields were obtained when the same reaction was performed while utilizing DMF instead of  $\text{CHCl}_3$  (entry 2). A closer examination illustrated that when the DMF was replaced with acetone, the yield was markedly improved (entry 3). Replacement of acetone with ethyl acetate (entry 4) did not give an improved result, while the formation of product 1a, was drastically increased when using the same catalyst in acetonitrile at reflux condition (entry 5). In contrast, utilizing EtOH and  $\text{H}_2\text{O}$ , evidently gave the desired product in lower yields (entries 6 and 7). Surprisingly, highest yield (92%) was obtained when the same reaction was carried out while utilizing a catalytic amount (10 mg) of Cu@imineZCMNPs at 80 °C under solvent-free conditions (entry 8). In the next phase of study, the effect of catalyst loading on the completion of the reaction was also investigated (entries 9–12). As shown, the best result was obtained for 10 mg loading (entry 8). After further survey, it was also observed that the use of heating with the

same amount of catalyst (10 mg) can also be greatly affected in this transformation (entries 14–16). It is essential to mention that the desired product could not be identified at room temperature (entry 13). In addition, control experiments demonstrated that any formation of the desired product 1a, was obtained in the absence of the catalyst under solvent-free conditions, even at 100 °C (entries 17 and 18).

After the successful generation of 1a, a variety of appropriate aldehydes (2a–q) were selected for the reaction acetophenone, malononitrile and ammonium acetate in the presence of Cu@imineZCMNPs at 80 °C under solvent-free condition, and desired 2-amino-3-cyanopyridine derivatives were achieved in good to high yields without problems which may be relevant to the use of solvents such as pollution, handling and safety. The optimized results are summarized in Table 2. The electronic effect seemed to have a clear influence on the reaction since aromatic aldehydes with electron-donating groups (entries 12–15) illustrated relatively low reactivity compared to the electron-withdrawing and heteroaromatic groups (entries 2–11 and 16–17).

In a proposed mechanism, as depicted in Scheme 2. The reaction may proceed via enamine 3, which generated from the reaction of acetophenone and ammonium acetate, and then activated by  $\text{Cu}^{2+}$  cation, reacts with alkylidenemalononitrile 2 (generated from the reaction of aldehyde and malononitrile) to yield the corresponding intermediate 4, followed by tautomerization and cycloaddition to give intermediate 6 which could isomerize and aromatize to afford the final product.

In the next phase of the study, the recovery and reuse cycle of Cu@imineZCMNPs was also investigated. Hence, we surveyed the recyclability of Cu@imineZCMNPs for five consecutive cycles to afford the synthesis of 2-amino-4,6-diphenyl-nicotinonitrile (1a). As shown in Fig. 8, this nanocatalyst can be recycled at least five times with a negligible decrease in the catalytic activity, and the yields ranged from 92 to 87%.

**Table 1** Optimization of the reaction conditions in different solvents

Entry	Solvent	Amount of catalyst (mg)	Temperature (°C)	Reaction time (h)	Yield (%) <sup>a</sup>
1	CHCl <sub>3</sub>	10	Reflux	1	18
2	DMF	10	Reflux	1	45
3	Acetone	10	Reflux	1	68
4	Ethyl acetate	10	Reflux	1	63
5	Acetonitrile	10	Reflux	1	85
6	EtOH	10	Reflux	1	23
7	H <sub>2</sub> O	10	Reflux	1	15
8	–	10	80	18 min	92
9	–	5	80	18 min	82
10	–	8	80	18 min	90
11	–	12	80	18 min	94
12	–	15	80	18 min	93
13	–	10	25	18 min	36
14	–	10	50	18 min	60
15	–	10	60	18 min	76
16	–	10	70	18 min	88
17	–	–	25	18 min	–
18	–	–	100	18 min	–

Reaction conditions: a mixture of benzaldehyde (1 mmol), acetophenone (1 mmol), malononitrile (1 mmol), ammonium acetate (1.5 mmol) and Cu@imineZCMNPs (10 mg)

<sup>a</sup>Isolated yield

**Table 2** Synthesis of 2-amino-4,6-diphenylnicotinonitrile derivatives in the presence of the Cu@imineZCMNPs

Entry	Product	R	Yield <sup>a</sup> (%)	Time (min)	Mp <sup>b</sup> (°C) found	Mp (°C) (Lit)
1	1a	C <sub>6</sub> H <sub>5</sub> -	92	18	185–187	186–187 [26]
2	1b	2-(Cl)-C <sub>6</sub> H <sub>4</sub> -	95	13	190–192	193–196 [27]
3	1c	4-(Cl)-C <sub>6</sub> H <sub>4</sub> -	95	13	170–172	169–171 [28]
4	1d	2,4-(Cl) <sub>2</sub> -C <sub>6</sub> H <sub>3</sub> -	92	18	239–241	243–245 [28]
5	1e	3-(Br)-C <sub>6</sub> H <sub>4</sub> -	91	18	164–166	165–167 [28]
6	1f	4-(Br)-C <sub>6</sub> H <sub>4</sub> -	93	18	213–216	215–218 [29]
7	1g	4-(F)-C <sub>6</sub> H <sub>4</sub> -	95	12	211–214	210–213 [28]
8	1h	3-(NO <sub>2</sub> )-C <sub>6</sub> H <sub>4</sub> -	92	13	190–192	190–193 [28]
9	1i	4-(NO <sub>2</sub> )-C <sub>6</sub> H <sub>4</sub> -	96	12	210–212	212–213 [26]
10	1j	4-(CN)-C <sub>6</sub> H <sub>4</sub> -	96	12	189–191	184–186 [30]
11	1k	4-(CO <sub>2</sub> Me)-C <sub>6</sub> H <sub>4</sub> -	92	18	202–204	204–205 [31]
12	1l	2-(OCH <sub>3</sub> )-C <sub>6</sub> H <sub>4</sub> -	87	23	198–200	199–201 [28]
13	1m	3-(OCH <sub>3</sub> )-C <sub>6</sub> H <sub>4</sub> -	85	25	145–147	137–140 [28]
14	1n	4-(OCH <sub>3</sub> )-C <sub>6</sub> H <sub>4</sub> -	88	23	178–180	181–182 [26]
15	1o	4-(CH <sub>3</sub> )-C <sub>6</sub> H <sub>4</sub> -	86	23	216–219	224–227 [28]
16	1p	4-(pyridyl)-	94	15	213–216	215–218 [29]
17	1q	3-(thiophene)-	95	13	212–215	213–214 [31]

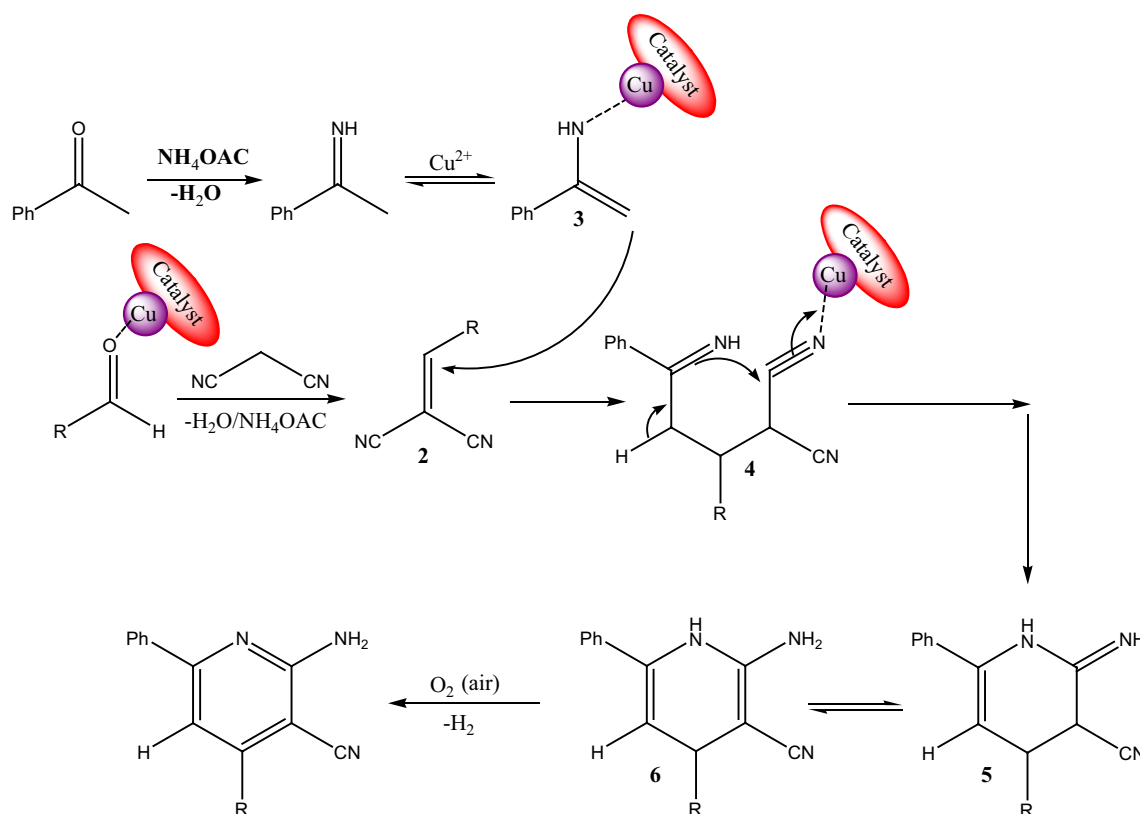
Reaction conditions: aldehyde (1 mmol), acetophenone (1 mmol), malononitrile (1 mmol) and ammonium acetate (1.5 mmol) and Cu@imineZCMNPs (10 mg), 80 °C

<sup>a</sup>Isolated yield

<sup>b</sup>Melting points are uncorrected

Furthermore, the catalytic efficiency and the capability of Cu@imineZCMNPs with some of the other previously

explored methods were compared with those of other methodologies which have been reported using other earlier



**Scheme 2** A proposed mechanistic pathway for the synthesis of 2-amino-3-cyanopyridines in presence of Cu@imineZCMNPs

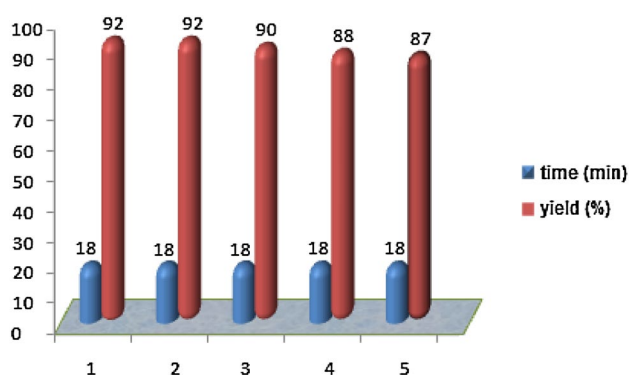


**Fig. 8** Reusability of the catalyst

homogeneous and heterogeneous catalysts for the synthesis of 2-amino-4,6-diphenylnicotinonitrile derivatives (Table 3). It is obvious that the reported protocol benefits from more advantages such as the lack of need for using toxic solvents, one step pathway and also low reaction time with high yields under solvent-free conditions.

## 4 Conclusion

In conclusion, we have reported a simple, facile, and efficient protocol the construction of a wide range of biologically and pharmacologically active 2-amino-3-cyanopyridine in the

**Table 3** Comparison the results of the synthesis of 3,4-dihydro-5-etoxy carbonyl-4-(4-phenyl)-6-methylpyrimidine-2(1H)-one using different catalysts

Entry	Catalyst and conditions	Reaction time (h)	Yield (%) <sup>b</sup>	Refs.
1	Nano Fe <sub>3</sub> O <sub>4</sub> /solvent-free/80 °C	2	90	[26]
2	Cellulose-SO <sub>3</sub> H /water/60 °C	2.5	95	[32]
3	Bu <sub>4</sub> N <sup>+</sup> Br <sup>-</sup> /water/reflux	2	92	[33]
4	Yb(PFO)/EtOH/reflux	4	90	[34]
5	FePO <sub>4</sub> /EtOH/reflux	4	93	[35]
6	Trifluoroethanol (TFE)/reflux	6	90	[36]
7	Cu@imineZCMNPs/solvent-free/80 °C	18 min	92	This work



presence of Cu@imineZCMNPs as a novel, environmentally friendly and reusable heterogeneous catalyst via a direct one-pot method starting from aldehydes, acetophenone, malononitrile, and ammonium acetate under solvent-free conditions.

## 5 Experimental

All chemical materials were purchased from Merck chemical company and used without further purification. The purity determination of the product and reaction monitoring were carried out using a TLC on silica gel PolyGram SILG/UV 254 plates. The melting points were measured with an Electrothermal 9100 apparatus and are uncorrected. Fourier transform infrared (FT-IR) spectra were recorded as KBr pellets on a PerkinElmer PXI instrument. The broad angle X-ray diffraction (XRD) measurements were accomplished using Ni-filtered Co K $\alpha$  radiation on a Siemens D-500 X-ray diffractometer (Germany) in the  $2\theta$  range of 10–80°. Scanning electron micrographs (SEM) of the samples were taken with SEM-LEO 1430VP. Thermogravimetric analysis (TGA) was made on a Linseis SATPT 1000 thermoanalyzer instrument. Samples were heated from 25 to 650 °C using a rate of 10 °C min<sup>-1</sup> under N<sub>2</sub> atmosphere. Magnetic susceptibility measurements were accomplished using a vibrating sample magnetometer (VSM/AGFM, MDK Co, Ltd, Iran) in the magnetic field range of – 8000 Oe to 8000 Oe at room temperature. Inductively coupled plasma atomic emission spectrometry (ICP-AES) measurements were carried out with VARIAN VISTA-MPX. Elemental analyses were done on a Carlo-Erba EA1110CNNO-S analyzer and agreed (within 0.30) with the calculated values.

### 5.1 Preparation of Fe<sub>3</sub>O<sub>4</sub> Nanoparticles (MNPs)

Fe<sub>3</sub>O<sub>4</sub> MNPs were synthesized using traditional chemical co-precipitation method. Typically, 2.36 g of FeCl<sub>3</sub>·6H<sub>2</sub>O and 0.86 g of FeCl<sub>2</sub>·4H<sub>2</sub>O were dissolved in 40 mL distilled water under stirring at 90 °C and continuous flow of argon gas. Thereafter, under rapid mechanical stirring, 10 mL of ammonia (25%) was added drop-wise to the reaction mixture. The resulting black MNPs were magnetically separated and washed the resulting black MNPs were magnetically separated with deionized water and dried at 60 °C for 12 h.

### 5.2 Preparation of Fe<sub>3</sub>O<sub>4</sub>@ZrO<sub>2</sub> Nanoparticles (ZCMNPs)

Zirconium (IV) oxychloride octahydrate (ZrOCl<sub>2</sub>·8H<sub>2</sub>O) (1 g) was dissolved in 50 mL of ethanol to form a clear solution and kept at 70 °C for 2 h. Then, Fe<sub>3</sub>O<sub>4</sub> MNPs (5 g) was added to that solution and the mixture was stirred with the

help of ultrasonication for 1 h and then was stirred for 12 h. After this period of time, the reaction mixture filtrated and 300 mL ethanol was added to filtrated solution to precipitate core-shell Fe<sub>3</sub>O<sub>4</sub>@ZrO<sub>2</sub> nanoparticles. Finally, the resulting precipitate was dried under vacuum oven.

### 5.3 Functionalization of Fe<sub>3</sub>O<sub>4</sub>@ZrO<sub>2</sub> with 3-aminopropyltriethoxysilane (AmpZCMNPs)

Core-shell Fe<sub>3</sub>O<sub>4</sub>@ZrO<sub>2</sub> nanoparticles (1 g) were dispersed in dry toluene (20 mL) for 20 min using ultrasound and then 3-aminopropyltriethoxysilane (Amp, 2 mL) was added to the resulting mixture. The mixture was refluxed for 24 h under argon atmosphere. After 24 h, the functionalized magnetite nanoparticles (MNP-AP) were separated from the reaction mixture using a permanent magnet, washed several times with ethanol and distilled water, and dried under vacuum oven.

### 5.4 Functionalization of AmpZCMNPs with Salicylaldehyde (imineZCMNPs)

To prepare imineZCMNPs, AmpZCMNPs (2 g) was dispersed in 20 mL of dry CH<sub>2</sub>Cl<sub>2</sub> for 30 min. After that, 0.245 g of salicylaldehyde was added to the reaction mixture and the mixture was refluxed for 6 h. Finally, these precipitates were separated by filtration, washed with 20 mL of water, and then dried under vacuum oven.

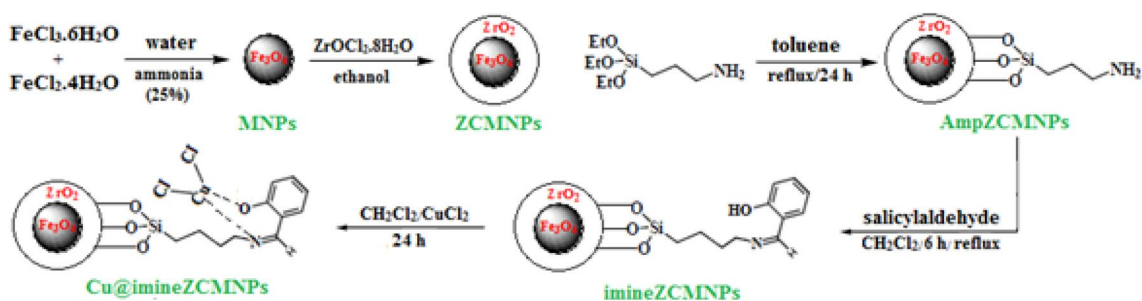
### 5.5 Preparation of Cu@imineZCMNPs

Two grams of imineZCMNPs was suspended in 20 mL of CH<sub>2</sub>Cl<sub>2</sub>. Thereafter, CuCl<sub>2</sub> (0.25 mmol) was added to CH<sub>2</sub>Cl<sub>2</sub> (10 mL), and the reaction mixture was stirred for 24 h under argon atmosphere. After 24 h, the resultant precipitate formed was separated by filtration, and the product was washed with water to remove unreacted metal precursors. All stages of the Cu@imineZCMNPs synthesis are shown in Scheme 3.

### 5.6 Selected Spectral Data

#### 5.6.1 2-Amino-4,6-Diphenylnicotinonitrile (1a)

Yield: 92%; White solid; m.p. 185–187 °C; <sup>1</sup>H NMR (400 MHz, CDCl<sub>3</sub>, ppm):  $\delta$  8.11 (s, 2H), 7.48 (m, 8H), 7.32 (s, 1H), 7.12 (s, 2H); <sup>13</sup>CNMR (100 MHz CDCl<sub>3</sub>, ppm): 158.7, 155.2, 151.3, 138.9, 135.4, 127.6, 125.8, 123.1, 122.7, 121.9, 120.8, 119.7, 107.4, 84.5; FT-IR (KBr, cm<sup>-1</sup>): 3429, 3312, 3159, 2215, 1632, 1559, 1456, 1368, 1241, 751, 683. ESI-HRMS [M+H]<sup>+</sup>*m/z* Found: 271.1152. C<sub>18</sub>H<sub>13</sub>N<sub>3</sub> Calculated: 271.1138.



**Scheme 3** Synthesis of Cu@imineZCMNPs

### 5.6.2 2-Amino-4-(2-Chlorophenyl)-6-Phenylnicotinonitrile (1b)

Yield: 95%; White solid; m.p. 190–192 °C;  $^1\text{H}$  NMR (400 MHz,  $\text{CDCl}_3$ , ppm):  $\delta$  8.05 (s, 2H), 7.45 (s, 4H), 7.32 (s, 1H), 7.16 (s, 2H), 7.07 (s, 1H), 6.89 (s, 2H);  $^{13}\text{C}$  NMR (100 MHz  $\text{CDCl}_3$ , ppm): 158.3, 155.2, 154.1, 152.5, 135.4, 129.8, 129.7, 127.4, 126.9, 125.2, 124.7, 119.4, 115.2, 111.4, 109.7, 84.3, 56.11; FT-IR (KBr,  $\text{cm}^{-1}$ ): 3435, 3327, 2221, 1634, 1543, 1439, 1368, 1241, 751, 683. ESI-HRMS  $[\text{M} + \text{H}]^+ m/z$  Found: 305.0707.  $\text{C}_{18}\text{H}_{12}\text{ClN}_3$  Calculated: 305.0756.

### 5.6.3 2-Amino-4-(3-nitrophenyl)-6-phenylnicotinonitrile (1h)

Yield: 92%; Yellow solid; m.p. 190–192 °C;  $^1\text{H}$  NMR (400 MHz,  $\text{CDCl}_3$ , ppm):  $\delta$  8.18 (s, 2H), 7.49 (s, 4H), 7.27–7.34 (m, 3H), 7.06–7.16 (m, 3H);  $^{13}\text{C}$  NMR (100 MHz  $\text{CDCl}_3$ , ppm): 161.2, 160.1, 159.4, 155.2, 139.4, 136.8, 130.4, 128.2, 127.3, 126.4, 119.3, 118.1, 116.9, 111.7, 107.4, 83.1, 54.2; FT-IR (KBr,  $\text{cm}^{-1}$ ): 3432, 3310, 3162, 2200, 1627, 1549, 1535, 1248, 860, 755, 685. ESI-HRMS  $[\text{M} + \text{H}]^+ m/z$  Found: 317.2148.  $\text{C}_{18}\text{H}_{12}\text{N}_4\text{O}_2$  Calculated: 316.1089.

**Acknowledgements** We gratefully acknowledge financial support of this work by the Research Council of the University of Guilan.

## References

- Amali AJ, Rana RK (2009) *Green Chem* 11:1781
- Hu J, Wang Y, Han M, Zhou Y, Jiang X, Sun P (2012) *Catal Sci Technol* 2:2332
- Zhang Q, Su H, Luo J, Wei Y (2013) *Catal Sci Technol* 3:235
- Shylesh S, Wang L, Thiel WR (2010) *Adv Synth Catal* 352:425
- Cheng T, Zhang D, Li H, Liu G (2014) *Green Chem* 16:3401
- Gawande MB, Luque R, Zboril R (2014) *ChemCatChem* 6:3312
- Murata T, Shimada M, Sakakibara S, Yoshino T, Kadono H, Masuda T, Shimazaki M, Shintani T, Fuchikami K, Sakai K, Inbe H, Takeshita K, Niki T, Umeda M, Bacon KB, Ziegelbauer KB, Lowinger TB (2003) *Bioorg Med Chem Lett* 13:913
- Hammam AG, El-Hafez NAA, Midura WH, Mikolajczyk M, Naturforsch Z (2000) B: *J Chem Sci* 55:417
- Mantri M, De Graaf O, Van Veldhoven J, Göblyös A, Von Frittag Drabbe Künzel JK, Mulder-Krieger T, Link R, De Vries H, Beukers MW, Brussee J, Ijzerman AP (2008) *J Med Chem* 51:4449
- Gholap AR, Toti KS, Shirazi F, Kumari R, Bhat MK, Deshpande MV, Srinivasan KV (2007) *Bioorg Med Chem* 15:6705
- Deng J, Sanchez T, Al-Mawsawi LQ, Dayam R, Yunes RA, Garofalo A, Bolger MB, Neamati N (2007) *Bioorg Med Chem* 15:4985
- Vyas DH, Tala SD, Akbari JD, Dhaduk MF, Joshi KA, Joshi HS (2009) *Ind J Chem Sect B* 48:833
- Baldwin JJ, Engelhardt EL, Hirschmann R, Ponticello GS, Atkinson JG, Wasson BK, Sweet CS, Scriabine A (1980) *J Med Chem* 23:65
- Zhang F, Zhao Y, Sun L, Ding L, Gu Y, Gong P (2011) *Eur J Med Chem* 46:3149
- Girgis AS, Kalmouch A, Hosni HM (2004) *Amino Acids* 26:139
- Kambe S, Saito K (1980) *Synthesis* 1980:366
- Shi F, Tu S, Fang F, Li T (2005) *Arkivoc* I:137
- Tu SJ, Jiang H, Zhuang QY, Miao CB, Shi DQ, Wang XS, Gao YC (2003) *Chin J Org Chem* 23:488
- Zhou WJ, Ji SJ, Shen ZL (2006) *J Organomet Chem* 691:1356
- Yousefi H, Yahyazadeh A, Yazdanbakhsh MR, Rassa M, Moradi-eRufchahi EO (2012) *J Mol Struct* 1015:27
- Yousefi H, Yahyazadeh A (2012) *Chin Chem Lett* 23:685
- Yousefi H, Yahyazadeh A, Moradi-eRufchahi EO, Rassa M (2013) *J Mol Liq* 180:51
- Abbaspour-Gilandeh E, Aghaei-Hashjin M, Yahyazadeh A, Salemi H (2016) *RSC Adv* 6:55444
- Sheykhan M, Yahyazadeh A, Ramezani L (2017) *Mol Catal* 435:166
- Safari J, Zarnegar Z, Heydarian M (2012) *Bull Chem Soc Jpn* 85:1332
- Heravi MM, Beheshtiha SYS, Dehghani M, Hosseintash N (2015) *J Iran Chem Soc* 12:2075
- Khaksar S, Yaghoobi M (2012) *J Fluorine Chem* 142:41
- Zolfigol MA, Yarie M (2016) *Appl Organomet Chem* 1
- Safari J, Banitaba SH, Dehghan-Khalili S (2012) *Ultrason Sonochem* 19:1061
- Zolfigol MA, Khazaei A, Alaie S, Bagheri S, Maleki F, Bayat Y, Asgari A (2016) *RSC Adv* 6:58667
- Khalifeh R, Ghamari M (2016) *J Braz Chem Soc* 27:759



32. Mansoor SS, Aswin K, Logaiya K, Sudhan PN, Malik S (2014) *Res Chem Intermed* 40:871
33. Kurumurthy C, Naresh Kumar R, Yakaiah T, Shanthan Rao P, Narsaiah B (2015) *Res Chem Intermed* 41:3193
34. Tang J, Wang L, Yao Y, Zhang L, Wang W (2011) *Tetrahedron Lett* 52:509
35. Zadpour M, Behbahani FK (2015) *Monatsh Chem* 146:1865
36. Ghorbani-Vaghei R, Toghræi-Semiromi Z, Karimi-Nami R (2013) *C R Chim* 16:1111